PHYSICAL REVIEW D **93,** 105001 (2016)

Quark mass effect on axial charge dynamics

Er-dong Guo[1,3,*] and Shu Lin[2,†]

[1]*State Key Laboratory of Theoretical Physics, Institute of Theoretical Physics, Chinese Academy of Sciences, Beijing 100190, China*

[2]*Institute of Astronomy and Space Sciences, Sun Yat-Sen University, No 135 Xingang Xi Rd, Guangzhou 510275, China*

[3]*Kavli Institute of Theoretical Physics China, Chinese Academy of Sciences, Beijing 100190, China*

(Received 22 February 2016; published 2 May 2016)

We studied the effect of finite quark mass on the dynamics of the axial charge using the D3/D7 model in holography. The mass term in the axial anomaly equation affects both the fluctuation (generation) and dissipation of the axial charge. We studied the dependence of the effect on quark mass and an external magnetic field. For axial charge generation, we calculated the mass diffusion rate, which characterizes the helicity flipping rate. The rate is a nonmonotonous function of mass and can be significantly enhanced by the magnetic field. The diffusive behavior is also related to a divergent susceptibility of the axial charge. For axial charge dissipation, we found that in the long time limit, the mass term dissipates all the charge effectively generated by parallel electric and magnetic fields. The result is consistent with a relaxation time approximation. The rate of dissipation through mass term is a monotonous increasing function of both quark mass and a magnetic field.

DOI: 10.1103/PhysRevD.93.105001

I. INTRODUCTION

It is believed that parity odd domains with chiral imbalance are produced in finite temperature quark-gluon plasma (QGP). Their presence can be detected via an axial anomaly as a chiral magnetic effect (CME) [1–4] and chiral magnetic wave (CMW) [5,6] in heavy ion collisions; see Refs. [7–9] for recent reviews. The former leads to the generation of a vector current along the direction of the external magnetic field,

$$\vec{j}_V = \frac{N_c e}{2\pi^2}\mu_5 \vec{B}, \tag{1}$$

where μ_5 is the axial chemical potential characterizing the chiral imbalance. The latter leads to the propagation of axial and vector charges along the direction of the external magnetic field. Analogous effects exist when the magnetic field is replaced by vorticity of the QGP [10,11]. These effects have been intensively searched for in heavy ion collision experiments in recent years [12–14].

Theoretical descriptions of the CME and CMW have been developed in different frameworks including hydrodynamics [10,15–18], kinetic theory [19–25], etc. Most frameworks assume quarks being massless; see the exception, for example, in Refs. [26,27]. While it is known that finite quark mass does not modify the CME, we do expect the quark mass to have imprints on the dynamics of the axial charge. Naively, if the mass of one quark flavor is much larger than the temperature of the QGP, that quark flavor decouples from the axial current. We would like to ask quantitative questions about the mass effect on the dynamics of the axial charge. This is relevant in reality because the mass of the strange quark is comparable to the temperature of the QGP created at the Relativistic Heavy Ion Collider (RHIC) and LHC. With the inclusion of the mass term, the axial anomaly equation reads

$$\partial_\mu j_5^\mu = 2im\bar{\psi}\gamma^5\psi - \frac{e^2}{16\pi^2}\epsilon^{\mu\nu\rho\sigma}F_{\mu\nu}F_{\rho\sigma} - \frac{g^2}{16\pi^2}\mathrm{tr}\epsilon^{\mu\nu\rho\sigma}G_{\mu\nu}G_{\rho\sigma}, \tag{2}$$

where the three terms on the rhs correspond to the mass term, QED anomaly term, and QCD anomaly term, respectively. Equation (2) is written for one flavor of quark with mass m. All three terms lead to the modification of axial charge dynamics. The effect of the QED anomaly term is extensively studied in the above-mentioned references. The effect of the QCD anomaly was studied recently [28–31]. In this work, we will focus on the effect of the mass term. On one hand, finite quark mass explicitly breaks axial symmetry, offering a mechanism of axial charge generation. We find that the mass operator diffuses at low frequency the same way as the Chern-Simon (CS) number. The diffusion of the CS number is known to generate an axial charge. The same is true for the mass operator. We calculate the diffusion rate of the mass term as a measure of axial charge generation. We also define a dynamical susceptibility by the CME and find it to be divergent in the

*guoerdong@itp.ac.cn
†linshu8@mail.sysu.edu.cn

low frequency limit. We explain the common physical reason for the diffusive mass operator and the divergent susceptibility. On the other hand, finite quark mass also leads to axial charge dissipation. The dissipation effect was studied recently in Refs. [32,33] in a relaxation time approximation. We will discuss axial charge dissipation in an indirect way: we set up a parallel electric and magnetic field and measure the rate of dissipation through the mass term. The situation is further complicated by the existence of a reservoir of adjoint matter, to which the axial charge can dissipate. By taking into account the additional loss rate, we find that the axial charge dissipates entirely in the long time limit, which is consistent with the relaxation time approximation. We will study these effects as a function of both the quark mass and external magnetic field using a holographic model.

The paper is organized as follows. In Sec. II, we give a self-contained review of the holographic model. In Sec. III, we discuss separately the mass effect on axial charge generation and dissipation, which we coined the mass diffusion rate and mass dissipation effect, respectively. We summarize the results in Sec. IV. We collect technical details in obtaining the phase diagram and hydrodynamic solutions in two Appendixes.

II. QUICK REVIEW OF THE MODEL

A. D3/D7 background

We use the D3/D7 model to study the effect of the finite quark mass. The background is sourced by N_c D3 branes. The world volume fields of D3 branes are $\mathcal{N}=4$ supersymmetric Yang-Mills theory. In addition, there are N_f D7 branes in the background. The open string stretching between D3 and D7 branes is dual to the $\mathcal{N}=2$ hypermultiplet. The $\mathcal{N}=4$ and $\mathcal{N}=2$ fields are in the adjoint and fundamental representations of the $SU(N_c)$ group, respectively. By analogy with QCD, we will loosely refer to the $\mathcal{N}=4$ and $\mathcal{N}=2$ fields as gluons and quarks, respectively. A detailed account of the field content can be found in Ref. [34]. The $\mathcal{N}=4$ theory has a $SO(6)_R$ global symmetry, which is broken by the $\mathcal{N}=2$ theory to $SO(4)\times U(1)_R$. As we will see, the $U(1)_R$ symmetry is anomalous. We will identify it with axial symmetry. We start with the finite temperature black hole background of D3 branes following the notations of Ref. [35],

$$\begin{aligned} ds^2 &= g_{tt}dt^2 + g_{xx}d\vec{x}^2 + g_{\rho\rho}d\rho^2 \\ &\quad + g_{\theta\theta}d\theta^2 + g_{\phi\phi}d\phi^2 + g_{SS}d\Omega_3^2, \\ &= -\frac{r_0^2}{2}\frac{f^2}{H}\rho^2 dt^2 + \frac{r_0^2}{2}H\rho^2 dx^2 + \frac{d\rho^2}{\rho^2} \\ &\quad + d\theta^2 + \sin^2\theta d\phi^2 + \cos^2\theta d\Omega_3^2, \end{aligned} \tag{3}$$

where

$$f = 1-\frac{1}{\rho^4}, \qquad H = 1+\frac{1}{\rho^4}. \tag{4}$$

The temperature is fixed by $T=r_0/\pi$. Note that we have factorized S_5 into S_3 and two additional angular coordinates θ and ϕ, which makes the breaking of global symmetry $SO(6)_R \to SO(4)\times U(1)_R$ manifest. There is a nontrivial background Ramond-Ramond form

$$C_4 = \left(\frac{r_0^2}{2}\rho^2 H\right)^2 dt\wedge dx_1\wedge dx_2\wedge dx_3 - \cos^4\theta d\phi\wedge d\Omega_3. \tag{5}$$

In the probe limit $N_f/N_c \ll 1$, the D7 branes do not backreact on the background of the D3 branes. This corresponds to the quenched limit of QCD. The D3 and D7 branes occupy the following dimensions:

	x_0	x_1	x_2	x_3	x_4	x_5	x_6	x_7	x_8	x_9
D3	×	×	×	×						
D7	×	×	×	×	×	×	×	×		

. (6)

The D3 and D7 branes are separated in the x_8–x_9 plane. Using translation symmetry, we put D3 branes at the origin of the plane and parametrize the position of the D7 branes by radius $\rho\cos\theta$ and polar angle ϕ. The D7 branes have rotational symmetry in the x_8–x_9 plane, corresponding to $U(1)_R$ symmetry in the dual field theory. We use the symmetry to choose $\phi=0$. The embedding function $\theta(\rho)$ of the D7 branes in the D3 background is determined by minimizing the action including a Dirac-Born-Infeld (DBI) term and Wess-Zumino (WZ) term

$$\begin{aligned} S_{D7} &= S_{DBI} + S_{WZ}, \\ S_{DBI} &= -N_f T_{D7}\int d^8\xi\sqrt{-\det\left(g_{ab}+(2\pi\alpha')\tilde{F}_{ab}\right)}, \\ S_{WZ} &= \frac{1}{2}N_f T_{D7}(2\pi\alpha')^2\int P[C_4]\wedge\tilde{F}\wedge\tilde{F}. \end{aligned} \tag{7}$$

Here, T_{D7} is the D7 brane tension. g_{ab} and $\tilde{F}_{ab}$ are the induced metric and world volume field strength, respectively. Defining

$$\begin{aligned} F_{ab} &= (2\pi\alpha')\tilde{F}_{ab}, \\ \mathcal{N} &= N_f T_{D7}2\pi^2 = \frac{N_f N_c}{(2\pi)^4}, \end{aligned} \tag{8}$$

we simplify the action to

$$S_{DBI} = -\frac{\mathcal{N}}{2\pi^2}\int d^8\xi\sqrt{-\det\left(g_{ab}+F_{ab}\right)},$$
$$S_{WZ} = \frac{1}{4\pi^2}\mathcal{N}\int P[C_4]\wedge F\wedge F. \tag{9}$$

The mass of the quark is realized as the separation of the D7 branes from the D3 branes at infinity. Explicitly, the mass M is determined from the asymptotic behavior of θ,

$$\sin\theta = \frac{m}{\rho}+\frac{c}{\rho^3}+\cdots, \tag{10}$$

with $M = r_0 m$. We will turn on a constant magnetic field, which amounts to including a world volume magnetic field in D7 branes. There are two possible embeddings with D7 branes crossing/not crossing the black hole horizon, corresponding to the meson melting/mesonic phase, respectively [35–38]. Using t, $\vec{x}$, ρ, and angular coordinates on S_3 as world volume coordinates, the induced metric is given by

$$ds^2_{\rm ind} = -\frac{r_0^2}{2}\frac{f^2}{H}\rho^2 dt^2+\frac{r_0^2}{2}H\rho^2 d\vec{x}^2 + \left(\frac{1}{\rho^2}+\theta'(\rho)^2\right)d\rho^2+\cos^2\theta d\Omega_3^2. \tag{11}$$

We also turn on a constant magnetic field in the z direction: $F_{xy} = B$. The action of D7 branes can be written as

$$S_{DBI} = -\mathcal{N}\int d\rho\left(\frac{r_0^2}{2}\right)^2 fH\rho^3\sqrt{1+\rho^2\theta'^2} \times\sqrt{1+\frac{2B^2}{r_0^2 H\rho^2}}\cos^3\theta, \tag{12}$$

with a vanishing WZ term. The phase diagram in the $m-B$ plane has been obtained in Refs. [37,38]. We reproduce the result in Appendix A and show the result at fixed temperature in Fig. 1. The two phases are the mesonic phase with larger m and B and the meson melting phase with smaller m and B. In the former case, the R-charge (axial charge) exchange between fundamental matter and the adjoint sector is not possible due to the formation of a meson bound state, while in the latter case, the R charge (axial charge) can leak from fundamental matter to the adjoint sector. The phase diagram implies that a large quark mass and magnetic field favors the formation of a meson bound state. The effect of a magnetic field may be understood via an increased effective quark mass. We are interested in the meson melting phase, which is more relevant for application in QGP.

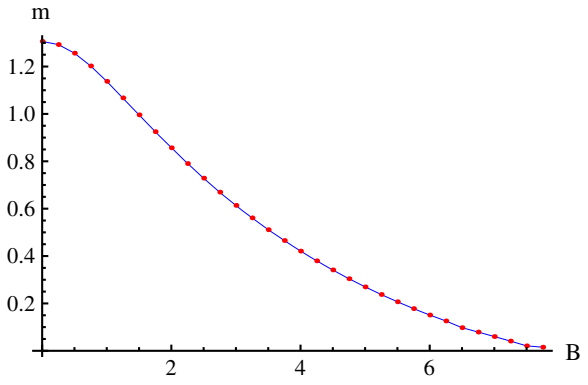

FIG. 1. $m-B$ phase diagram of the D3/D7 background. The axis labels are dimensionless numbers with units set by $\pi T = 1$. The region with small m and B corresponds to the meson melting phase, while the region with large m and B corresponds to the mesonic phase.

B. Fluctuations and realization of axial anomaly

We consider the fluctuation of the embedding function ϕ and world volume gauge field A_M. The quadratic action can be written in the following compact form,

$$S = \mathcal{N}\int d^5x\left(-\frac{1}{2}\sqrt{-G}G^{MN}\partial_M\phi\partial_N\phi-\frac{1}{4}\sqrt{-H}F^2\right) -\mathcal{N}\kappa\int d^5x\Omega\epsilon^{MNPQR}F_{MN}F_{PQ}\partial_R\phi, \tag{13}$$

where $M = t, x_1, x_2, x_3, \rho$. The equation of motion (EOM) of ϕ is given by

$$\frac{\delta S}{\delta\phi}-\partial_M\left(\frac{\delta S}{\delta\partial_M\phi}\right) = 0. \tag{14}$$

Since ϕ is a phase, only its derivative enters the action, and we have from (14)

$$\partial_\mu\left(\frac{\delta S}{\delta\partial_\mu\phi}\right)+\partial_\rho\left(\frac{\delta S}{\delta\partial_\rho\phi}\right) = 0, \tag{15}$$

with $\mu = t, x_1, x_2, x_3$. Defining $J^\mu_R = \int d\rho\frac{\delta S}{\delta\partial_\mu\phi}$, we obtain

$$\partial_\mu J^\mu_R+\left.\frac{\delta S}{\delta\partial_\rho\phi}\right|^\infty_{\rho=\rho_h} = 0. \tag{16}$$

We will identify J_R as the axial current. The nonconservation of J_R follows from two boundary terms in the integration. The boundary term at the horizon $\rho = \rho_h$ indicates axial charge exchange between D7 branes and D3 branes. It is pointed out in Ref. [34] that this term represents leakage of the R charge from the fundamental sector to the adjoint sector as fields in both sectors are charged under the $U(1)_R$ symmetry. The other boundary term at $\rho = \infty$ can be related to the axial anomaly,

$$O_\phi \equiv -\left.\frac{\delta S}{\delta\partial_\rho\phi}\right|_{\rho=\infty} = -\frac{\delta S^\partial}{\delta\phi(\rho\to\infty)}, \tag{17}$$

where we have used the defining property of the on-shell action S^∂. For action (13), we have

$$O_\phi = \mathcal{N}\sqrt{-G}G^{M\rho}\partial_M\phi|_{\rho=\infty} + \kappa\mathcal{N}\Omega\epsilon^{MNPQ}F_{MN}F_{PQ}|_{\rho=\infty}. \tag{18}$$

For our model,

$$\sqrt{-G}G^{MN} = \sqrt{-h}g^{MN}g_{\phi\phi}, \qquad \sqrt{-H} = \sqrt{-h},$$
$$\Omega = \cos^4\theta, \qquad \kappa = \frac{1}{8}, \tag{19}$$

with h to be defined in the next section. Field theory analysis shows that [34][1]

$$O_\phi = mi\bar\psi\gamma^5\psi + \cdots + \mathcal{N}E\cdot B, \tag{20}$$

where $\cdots$ represents the contribution from supersymmetric partners. Noting that $\theta\to 0$ as $\rho\to\infty$, we readily identify the second term in (18) with the last term in (20). The remaining term in (18) can then be identified with the mass term in (20). For convenience, we define the remaining term by

$$O_\eta = \mathcal{N}\sqrt{-G}G^{M\rho}\partial_M\phi|_{\rho=\infty}. \tag{21}$$

We have thus holographically split O_ϕ into the mass term O_η and anomaly term $\mathcal{N}E\cdot B$, which represent, respectively, the explicit and anomalous breaking of the axial symmetry:

$$\partial_\mu J^\mu_R = O_\phi = O_\eta + \mathcal{N}E\cdot B. \tag{22}$$

III. FINITE QUARK MASS EFFECT

We will study two aspects of the finite quark mass effect: (i) The mass term, similar to the QCD anomaly term, has diffusive behavior at low frequency. This gives rise to fluctuation (random walk behavior) of the axial charge. The rate of diffusion, to be referred to as the mass diffusion rate, determines the rate of axial charge generation. (ii) In the presence of nonvanishing $E\cdot B$, a net axial charge would be produced. However, the axial charge dissipates due to finite quark mass, resulting in a reduced rate of axial charge generation. We will refer to this as the mass dissipation effect. The above effects are captured by correlators of J^z and O_η. The mass diffusion rate involves the correlator of O_η itself, while the mass dissipation effect involves the correlator between J^z and O_η. We stress that J^z is the vector current coupled to the boundary gauge field A_z. In holographic formulation, we need to study the fluctuation of bulk fields A_z and ϕ, which are dual to J^z and $O_\eta(O_\phi)$. For our purpose, it is sufficient to turn on homogeneous (in both $\vec{x}$ and S_3) fluctuation of $A_z(t,\rho)$ and $\phi(t,\rho)$. The fluctuation leads to a modification to the following quantities:

$$ds^2_{\rm ind} = (g_{tt}+g_{\phi\phi}\dot\phi^2)dt^2 + g_{xx}dx^2 + (g_{\rho\rho}+g_{\theta\theta}\theta'^2+g_{\phi\phi}\phi'^2)d\rho^2 + g^2_{SS}d\Omega_3^2 + 2g_{\phi\phi}\dot\phi\phi' dtd\rho,$$
$$\delta F = \dot A_z dt\wedge dz + A_z' d\rho\wedge dz,$$
$$\delta P[C_4] = -\cos^4\theta(\dot\phi dt + \phi' d\rho)\wedge d\Omega_3. \tag{23}$$

With (23), we can write down the quadratic action of $A_z(t,\rho)$ and $\phi(t,\rho)$,

$$S_{\rm DBI}+S_{\rm WZ} = -\mathcal{N}\int dtd^3xd\rho\left[\frac{1}{2}\sqrt{-h}(g^{tt}g_{\phi\phi}\dot\phi^2 + g^{\rho\rho}g_{\phi\phi}\phi'^2 + g^{tt}g^{xx}\dot A_z^2 + g^{\rho\rho}g^{xx}A_z'^2) + \cos^4\theta B(\phi'\dot A_z - \dot\phi A_z')\right], \tag{24}$$

where we have defined

$$\sqrt{-h} = \sqrt{-g_{tt}g_{xx}(g_{xx}^2+B^2)(1+\rho^2\theta'^2)g_{\rho\rho}g_{SS}^3}. \tag{25}$$

Variation with respect to the fluctuations gives both the EOM and the on-shell action

$$\begin{aligned}\delta S = &-\mathcal{N}\int dtd^3xd\rho[\sqrt{-h}(-\partial_t(g^{tt}g_{\phi\phi}\dot\phi)\delta\phi - \partial_\rho(g^{\rho\rho}g_{\phi\phi}\phi')\delta\phi - \partial_t(g^{tt}g^{xx}\dot A_z)\delta A_z - \partial_\rho(g^{\rho\rho}g^{xx}A_z')\delta A_z)\\ &- \partial_\rho(\cos^4\theta B\dot A_z)\delta\phi + \partial_t(\cos^4\theta BA_z')\delta\phi - \partial_t(\cos^4\theta B\phi')\delta A_z + \rho(\cos^4\theta B\dot\phi)\delta A_z]\\ &-\mathcal{N}\int dtd^3x[\sqrt{-h}(g^{\rho\rho}g_{\phi\phi}\phi'\delta\phi + g^{\rho\rho}g^{xx}A_z'\delta A_z) + \cos^4\theta B(\dot A_z\delta\phi - \dot\phi\delta A_z)].\end{aligned} \tag{26}$$

[1]Note that we have $\phi = 0$, and thus no axial chemical potential is introduced.

Working with a single Fourier mode $e^{-i\omega t}$, we obtain the EOM

$$\begin{aligned}&\omega^2\sqrt{-h}g^{tt}g_{\phi\phi}\phi-\partial_\rho(\sqrt{-h}g^{\rho\rho}g_{\phi\phi}\phi')\\&\quad-B\partial_\rho(\cos^4\theta)A_z(-i\omega)=0,\\&\omega^2\sqrt{-h}g^{tt}g^{xx}A_z-\partial_\rho(\sqrt{-h}g^{\rho\rho}g^{xx}A_z')\\&\quad+B\partial_\rho(\cos^4\theta)\phi(-i\omega)=0.\end{aligned}\tag{27}$$

The asymptotic expansion of ϕ and A_z can be determined from the EOM:

$$\begin{aligned}\phi&=f_0+\frac{f_1}{\rho^2}+\frac{f_h}{\rho^2}\ln\rho+\cdots,\\A_z&=a_0+\frac{a_1}{\rho^2}+\frac{a_h}{\rho^2}\ln\rho+\cdots.\end{aligned}\tag{28}$$

f_0 and a_0 correspond to sources coupled to O_ϕ and J^z. The coefficients of the logarithmic terms correspond to counterterms[2]:

$$f_h=\frac{\omega^2}{r_0^2}f_0,\qquad a_h=\frac{\omega^2}{r_0^2}a_0.\tag{29}$$

The values of O_ϕ and J^z are determined by

$$\begin{aligned}O_\phi&=\frac{\delta S^\partial}{\delta\phi(\rho\to\infty)}\\&=(-\mathcal{N}\sqrt{-h}g^{\rho\rho}g_{\phi\phi}\phi'-\mathcal{N}\cos^4\theta B\dot{A}_z)|_{\rho\to\infty}\\&=2\mathcal{N}\left(\frac{r_0^2}{2}\right)^2m^2f_1-\mathcal{N}Ba_0(-i\omega),\\J^z&=\frac{\delta S^\partial}{\delta A_z(\rho\to\infty)}\\&=(-\mathcal{N}\sqrt{-h}g^{\rho\rho}g^{xx}A_z'+\mathcal{N}\cos^4\theta B\dot{\phi})|_{\rho\to\infty}\\&=2\mathcal{N}\left(\frac{r_0^2}{2}\right)a_1+\mathcal{N}Bf_0(-i\omega),\end{aligned}\tag{30}$$

where we have used $\rho\sin\theta|_{\rho\to\infty}=m$ according to (10). Comparing (21) and (30), we arrive at the following dictionary:

$$O_\eta=2\mathcal{N}\left(\frac{r_0^2}{2}\right)^2m^2f_1.\tag{31}$$

[2]Counterterms proportional to B^2 can in principle exist but are not found in this case.

A. Mass diffusion rate and susceptibility

The mass operator O_η can lead to fluctuation of the axial charge. It is well known that the origin of axial charge fluctuation from the QCD anomaly is topological transitions. The counterpart for O_η is helicity flipping from elementary scattering [39,40]. The rate of axial charge generation in the case of topological transition is given by the CS diffusion rate. Similarly, the corresponding rate in the case of helicity flipping is given by the diffusion rate of O_η, which we calculate below. The diffusion rate of O_η is encoded in the low frequency limit of the retarded correlator. To calculate the retarded correlator, we need to turn on the source for ϕ while keeping A_z vanishing on the boundary. Both ϕ and A_z satisfy the infalling wave condition on the horizon. It follows from (31) that the retarded correlator is given by

$$\begin{aligned}G_{\eta\eta}(\omega)&=\int dt\langle[O_\eta(t),O_\eta(0)]\rangle\Theta(t)e^{i\omega t}\\&=-2\mathcal{N}\left(\frac{r_0^2}{2}\right)^2m^2\frac{f_1}{f_0}.\end{aligned}\tag{32}$$

The diffusion rate is defined by

$$\Gamma_m=\lim_{\omega\to0}\frac{2iT}{\omega}G_{\eta\eta}(\omega).\tag{33}$$

For the case $B=0$, there is no mixing between ϕ and A_z. We can simply use $\phi^{(0)}$ (B2) in Appendix B:

$$\begin{aligned}\phi^{(0)}(\rho)=1-\frac{i\omega}{2r_0}\Bigg[&\int_1^\rho d\rho'\left(\frac{(\frac{r_0^2}{2})^2 8\cos^3\theta_h\sin^2\theta_h}{\sqrt{-h(\rho')}g^{\rho\rho}(\rho')g_{\phi\phi}(\rho')}-\frac{1}{\rho'-1}\right)\\&+\ln(\rho-1)\Bigg].\end{aligned}\tag{34}$$

This gives the following retarded correlator of O_η:

$$G_{\eta\eta}(\omega)=-2\mathcal{N}\left(\frac{r_0^2}{2}\right)^2\frac{i\omega}{4r_0}8\cos^3\theta_h\sin^2\theta_h.\tag{35}$$

Equation (35) gives a mass diffusion rate Γ_m as an analog of the CS diffusion rate:

$$\Gamma_m=\frac{\mathcal{N}}{\pi}\left(\frac{r_0^2}{2}\right)^2 8\cos^3\theta_h\sin^2\theta_h.\tag{36}$$

The dependence on m is encoded in the combination of trigonometric functions, which clearly indicates an upper bound of the mass diffusion rate. We also extract Γ_m using (33) with numerical solutions for general B and m in the meson melting phase. We plot the numerical results of Γ_m as a function of m^2 for different values of B in Fig. 2. The case $B=0$ agrees well with analytic expression (35). We

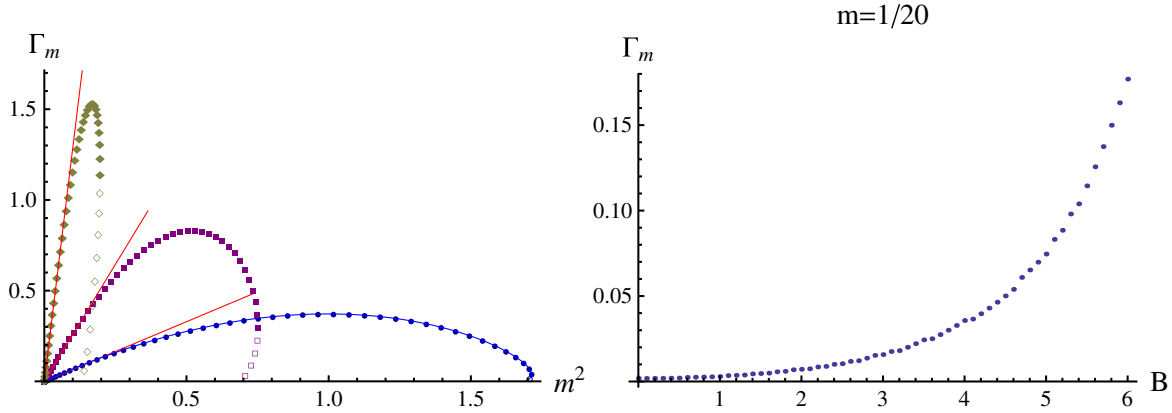

FIG. 2. (left) The mass diffusion rate Γ_m as a function of m^2 for $B=0$ (blue point), $B=2$ (purple square), and $B=4$ (brown diamond). The units are set by $\pi T=1$. The blue line is given by (36) which fits well for $B=0$. To guide the eyes, we also include linear fittings (red line) in the small mass region. The linear behavior is consistent with the field theory expectation. We have used empty symbols for points in metastable phases (right) Γ_m as a function of B at $m=1/20$. A rapid growth of Γ_m with B is found.

find the mass diffusion rate is a nonmonotonous function of m. This is not difficult to understand; in the limit $m\to 0$, Γ_m obviously should vanish as $O_\eta \sim m$. When m approaches the phase boundary between the meson melting phase and mesonic phase, we also expect helicity flipping to freeze due to the formation of meson bound states. In between, there must be a maximum for Γ_m. Furthermore, the linear behavior of the Γ_m–m^2 plot in the small m region supports the scaling $\Gamma_m \sim m^2$, which is consistent with the field theory expectation. The B dependence is more interesting: Γ_m shows rapid growth with B. The presence of B enhances the diffusion, which cannot be explained as the increase of effective mass. The enhancement of helicity flipping might provide a way to generate the axial charge more efficiently. It is worth mentioning that an enhancement of the CS diffusion rate due to the magnetic field was also obtained in Refs. [41,42].

We would like to comment on the diffusive behavior of O_η. On general ground, the mass diffusion effect leads to the accumulation of the axial charge, which prevents its further generation. It would lead to a modification of the long time (low frequency) behavior of $G^R_{\eta\eta}$. However, this does not happen due to the existence of the adjoint reservoir. The generated axial charge entirely dissipates to the adjoint reservoir. To see that, we compare O_η and $O_{\rm loss}$, which are the same quantity below evaluated at $\rho=\infty$ and $\rho=1$, respectively,

$$\mathcal{N}\sqrt{-h}g^{\rho\rho}\rho_{\phi\phi}\phi'. \tag{37}$$

It follows from the EOM (27) that the above quantity is constant in the limit $\omega\to 0$,

$$\partial_\rho(\mathcal{N}\sqrt{-h}g^{\rho\rho}\rho_{\phi\phi}\phi')=0, \tag{38}$$

meaning that the generated charge is entirely balanced by the loss to the reservoir. Consequently, the low frequency behavior of the O_η correlator is still diffusive.

Turing on the source for O_η also allows us to study the susceptibility of the axial charge. In the presence of finite quark mass, the axial charge is not even approximately conserved, making the susceptibility a subtle concept. Following Ref. [31], we can use the CME to define a dynamical susceptibility χ. In the present model, it is given by

$$\chi=\frac{n_5}{\mu_5}=\frac{\mathcal{N}Bn_5}{J^z}. \tag{39}$$

We need to calculate both n_5 and J^z from the response to the source for O_ϕ in the hydrodynamic limit. n_5 is essentially known already. Denoting the source by f_m, we can express n_5 as

$$\begin{aligned}-i\omega n_5(\omega)&=O_\eta(\omega)\\&=-G^R_{\eta\eta}(\omega)f_m(\omega)\sim O(\omega)f_m(\omega).\end{aligned} \tag{40}$$

Therefore, we obtain $n_5\sim O(\omega^0)f_m(\omega)$. On the other hand, J^z is calculated using the dictionary (30). It is generated through the mixing between ϕ and A_z. J^z is also expressible as a response to f_m,

$$J^z(\omega)=-G^R_{j\eta}(\omega)f_m(\omega). \tag{41}$$

Using the hydrodynamic solution (B11) in Appendix B and the dictionary (30), we find that there are two contributions to $G^R_{j\eta}$, both of which are of order $O(\omega B)$. Therefore, we have $J^z\sim O(\omega B)f_m(\omega)$. Plugging the above qualitative results into (39), we obtain

$$\chi \sim O(\omega^{-1}). \tag{42}$$

It simply means that the susceptibility is divergent in the static limit $\omega \to 0$. Recalling that the susceptibility is well defined in the massless limit, we arrive at the noncommutativity of the limits $m \to 0$ and $\omega \to 0$. The physical reason for the divergent susceptibility is not difficult to understand. On one hand, the mass diffusion effect can spontaneously generate axial charge density at the cost of no energy. On the other hand, as we have seen already, the adjoint reservoir is a perfect sink for the axial charge in the flavor sector, preventing the accumulation of the axial charge. Consequently, the axial charge can be continuously generated in the flavor sector. Note that the situation is different in the case of axial charge generation by the QCD anomaly. There, the breaking of axial symmetry is suppressed by $1/N_c$ (or the quenched limit), resulting in a finite dynamical susceptibility.

B. Mass dissipation effect

To study the mass dissipation effect, we turn on an electric field in the z-direction by a time dependent A_z on the boundary. We do not need to source ϕ on the boundary. Its profile is entirely generated via the mixing of A_z and ϕ in the bulk. The resulting O_η from the nontrivial profile of ϕ corresponds to the mass dissipation effect we are after. We also impose the infalling wave boundary condition for ϕ and A_z since we are interested in calculating the response. We define the dimensionless mass dissipation rate

$$r = \frac{O_\eta}{\mathcal{N} E \cdot B}. \tag{43}$$

The rate is a function of ω, m, and B. In the hydrodynamic limit $\omega \to 0$, we can show that $r(\omega \to 0)$ is a real function of m and B. In fact, it can be related to the embedding function for given m and B in the meson melting phase. To obtain $r(\omega \to 0)$ analytically, we need to solve the coupled EOM (27) in the hydrodynamic limit. The hydrodynamic solutions can be found in Appendix B. We simply quote the results here. The leading nontrivial order is the zeroth order for A_z and the first order for ϕ,

$$\begin{aligned} A_z^{(0)} &= a_0, \\ \phi^{(1)} &= \frac{(1-\cos^4\theta_h) B i \omega a_0}{(\frac{r_0^2}{2})^2 m^2 (-2)} \rho^{-2} + \cdots, \end{aligned} \tag{44}$$

where θ_h is the value of θ on the horizon, which needs to be obtained from the numerical embedding function for given m and B. For $\phi^{(1)}$, we only retain its asymptotic behavior relevant for extracting O_η. Equation (44) leads to the following rate:

$$r = 1 - \cos^4\theta_h. \tag{45}$$

We also study the rate of dissipation by numerical solutions. In practice, we generate two independent infalling numerical solutions at the horizon and use their linear combination to construct the solution with the desired boundary condition. We show the m dependence of r in the limit $B = 0$ and the B dependence of r at different values of m in Figs. 3 and 4. We find good agreement with analytic expression (45). On general ground, we expect the rate to be a monotonous increasing function of m. In particular, $r \to 0$ as $m \to 0$. Indeed, this is confirmed in Fig. 3. We further note that the effect of B enhances the dissipation on top of the mass effect in Fig. 4. The physical interpretation of the dissipation rate r turns out to be a subtle question. Recalling the axial anomaly equation (22), we would draw the following conclusion: for every one unit of axial charge generated by the parallel electric and magnetic field, an r

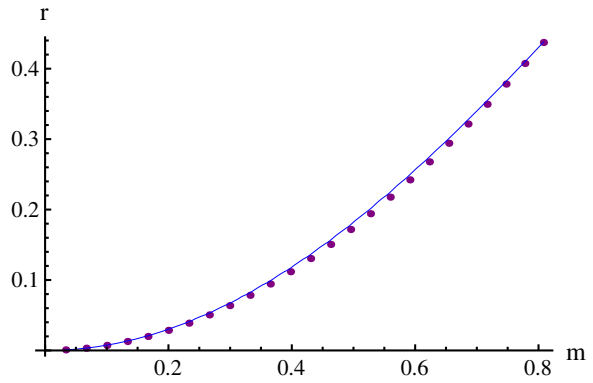

FIG. 3. The mass dissipation rate r as a function of m from numerics with small B and small ω. It is a monotonous increasing function of m as expected. The analytic function (45) is drawn in the blue line and fits the numerical results well. The units are set by $\pi T = 1$.

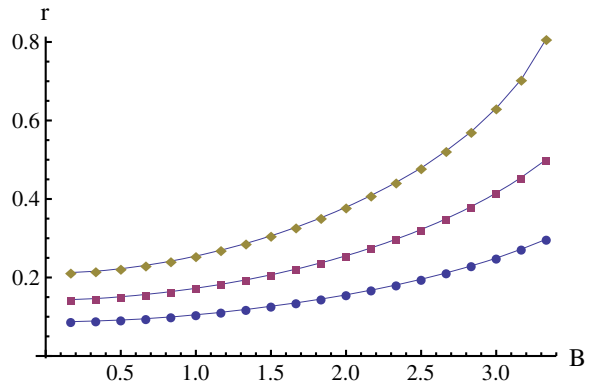

FIG. 4. The mass dissipation rate r as a function of B for $m = 7/20$ (blue point), $m = 9/20$ (purple square), and $m = 11/20$ (brown diamond). The units are set by $\pi T = 1$. The analytic function (45) is drawn in the blue line and fits the numerical results well. It is a monotonous increasing function of B.

unit of it dissipates through the mass term, with a unit of $1-r$ axial charge remaining. The remaining axial charge survives even in the hydrodynamic limit since we have $\omega \to 0$. This is not true because we have ignored a third source of axial charge dissipation, i.e., the loss to the adjoint reservoir. The anomaly equation (22) should be supplemented by the loss rate

$$\partial_\mu J_R^\mu = O_\eta + \mathcal{N} E \cdot B - O_{\rm loss}, \tag{46}$$

with the explicit form of the loss rate given by

$$O_{\rm loss} = \mathcal{N}\sqrt{-h} g^{\rho\rho} r_{\phi\phi} \partial_\rho \phi|_{\rho\to 1} + \mathcal{N}\Omega E \cdot B|_{\rho\to 1}. \tag{47}$$

It is known that the loss rate can be IR unsafe [43]. Indeed, plugging in the hydrodynamic solution $A_z^{(0)}$ and $\phi^{(1)}$ in Appendix B into (46), we find both terms become infinitely oscillatory as $\rho \to 1$. Nevertheless, we can still extract useful information by taking the hydrodynamic limit $\omega \to 0$ before the IR limit $\rho \to 1$. Using this regularization, we find the $\mathcal{N}\Omega E \cdot B$ term becomes $\mathcal{N}\cos^4\theta_h E \cdot B$, while the other term is higher order in ω. We immediately note that $\mathcal{N}\cos^4\theta_h E \cdot B$ is precisely the $1-r$ unit of axial charge. Subtracting the charge loss to the reservoir, we find only the r unit of axial charge is effectively generated in the flavor sector by the parallel electric and magnetic fields. All dissipate by the mass term. This simply means no axial charge survives in the hydrodynamic limit. After clarifying the role of the axial charge loss to the adjoint reservoir, we should interpret r as a measure of the mass dissipation effect compared to the dissipation to the adjoint reservoir. The dissipation through the mass term is favored at large m and B.

The statement on the nonsurvival of the axial charge can receive a correction higher order in ω, which quantifies the charge survival rate. We can compare with the relaxation time approximation employed in Refs. [32,33], in which the following form of the axial anomaly equation is assumed (here, the term $r\mathcal{N}E \cdot B$ corresponds to the axial charge generated effectively),

$$\partial_t n_5 = -\frac{n_5}{\tau} + r\mathcal{N} E \cdot B, \tag{48}$$

with τ being the relaxation time. Physically, it means the presence of the axial charge n_5 induces $O_\eta = -\frac{n_5}{\tau}$. Plugging it into (48), we can solve for O_η in the frequency space

$$O_\eta = -\frac{r\mathcal{N}E \cdot B}{1 - i\omega\tau}. \tag{49}$$

The leading order result $O_\eta = -r\mathcal{N}E \cdot B$ corresponds to our result of full dissipation. In principle, by going to high order in ω, we could calculate the relaxation time τ. We will not attempt it in this paper.

IV. SUMMARY

We have investigated the effect of the finite quark mass and magnetic field in the generation and dissipation of the axial charge, using a D3/D7 model. For axial charge generation, we calculated the mass diffusion rate. It is analogous to the Chern-Simon diffusion rate as a measure of axial charge fluctuation. The mass diffusion rate is a bounded nonmonotonous function of mass at vanishing magnetic field. The presence of the magnetic field enhances the diffusion. At small m, our numerical results are consistent with an approximate scaling for the mass diffusion rate,

$$\Gamma_m \sim m^2 F(B), \tag{50}$$

with $F(B)$ a rapid growing function in the meson melting phase. We also defined a dynamical susceptibility of the axial charge using the CME. We found the susceptibility to be divergent in the static limit $\omega \to 0$. It is due to two reasons: (i) spontaneous generation of the axial charge by the mass diffusion effect and (ii) continuous leakage of the axial charge from the flavor sector to the adjoint sector, preventing the accumulation of the axial charge.

For axial charge dissipation, we found that a mass term is induced in the presence of the parallel electric and magnetic fields, reducing the generation of the axial charge. After carefully subtracting the axial charge loss rate to the adjoint sector, we found that the axial charge dissipates entirely through the mass term in the long time limit. To the order we consider, it is consistent with a relaxation time approximation.

ACKNOWLEDGMENTS

We thank K. Landsteiner and Y. Yin for critical comments on an early version of the paper. We also thank D. Kharzeev, J. F. Liao, Y. Liu, L. Yaffe, H.-U. Yee, and Y. Yin for useful discussions. The work of S. L. is in part supported by Junior Faculty's Fund at Sun Yat-Sen University.

APPENDIX A: PHASE DIAGRAM AT FINITE m AND B

It is known that the D3/D7 brane system as a model for the finite temperature QGP in the quenched limit has a first order phase transition [35–38]. At a large quark mass and strong magnetic field (with the temperature fixed), the probe D7 brane lies outside of the black hole horizon. In this phase, the meson stays in the bound state, and its spectrum possesses a mass gap. At a small quark mass and weak magnetic field, the brane crosses the horizon, and this corresponds to the meson melting phase. The case in which

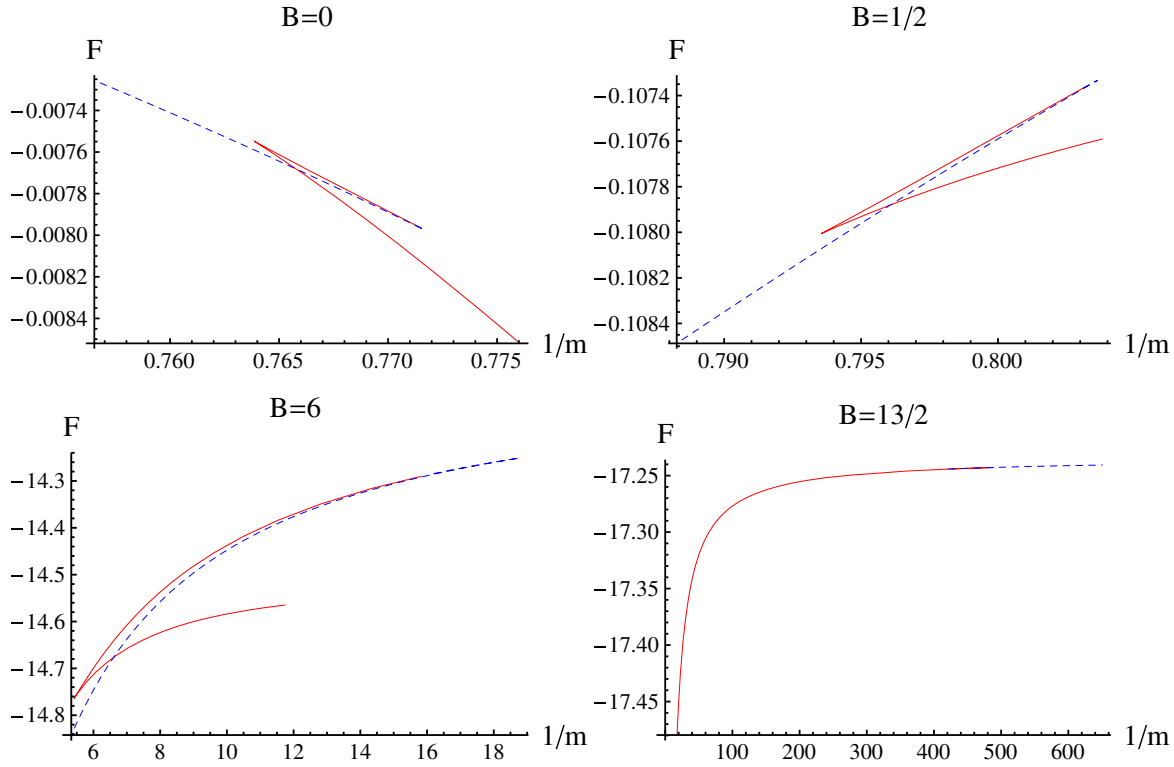

FIG. 5. Free energy F as a function of $1/m$ at different B for the D3/D7 system. The units are set by $\pi T = 1$. The red continuous (blue dashed) curves correspond to the black hole (Minkowski) embedding.

the D7 branes touch the horizon corresponds to critical embedding, giving rise to a critical mass and condensate. The embeddings close to the critical embedding show oscillatory behavior for the corresponding mass and condensate parameters around their critical values. This implies that the condensate is a multivalued function of mass, corresponding to different states. The true ground state is determined by the embedding that minimizes the free energy. Denoting $\chi = \sin\theta$, we can rewrite the action (12) as

$$S_{DBI} = -\mathcal{N}\int d\rho \frac{(1-\rho^4)(1-\chi^2)\sqrt{(1-\chi^2+\rho^2\chi'^2)(1+(2+4B^2)\rho^4+\rho^8)}}{4\rho^5}, \tag{A1}$$

where we have set $r_0 = 1$, which amounts to fixing the temperature $T = \frac{1}{\pi}$. The EOM following from (A1) is solved by numerical integration of the EOM. The black hole embedding and Minkowski embedding satisfy different boundary conditions. For black hole embedding, the boundary condition is $\chi(\rho = 1) = \chi_0, \chi'(\rho = 1) = 0$, with the integration domain from $\rho = 1$ to $\rho = \rho_{\max}$. For Minkowski embedding, the boundary condition is $\chi(\rho = \rho_{\min}) = 1, \chi'(\rho = \rho_{\min}) = \frac{(1-\rho^4)(1+(2+4B^2)\rho^4+\rho^8)}{\rho(1+\rho^4)(1+2B^2\rho^4+\rho^8)}$, with the integration domain from $\rho = \rho_{\min} > 1$ to $\rho = \rho_{\max}$. The initial condition for the derivative is chosen such that $\chi''(\rho = \rho_{\min})$ can be uniquely determined by the EOM. In practice, we start the integration at $\rho = 1 + \epsilon$ for black hole embedding and $\rho = \rho_{\min} + \epsilon$ for Minkowski embedding.

We note that the free energy $F = TS$ contains a UV divergence and therefore needs to be renormalized. Following Ref. [35], we add to the action the counterterm

$$S_{\text{counter}} = -\frac{\mathcal{N}}{4}\left[((\rho_{\max}^2 - m^2)^2 - 4mc) + \frac{B^2}{2}\ln\rho_{\max}\right]. \tag{A2}$$

Note the appearance of a new term due to the magnetic field as compared to Ref. [35]. The renormalized action $S = S_{DBI} + S_{\text{counter}}$ is finite as we take $\rho_{\max} \to \infty$. The true ground state is found by comparing the free energy of black hole embedding and Minkowski embedding, corresponding to the meson melting phase and mesonic phase. The phase transition is first order and is present only below a

certain critical magnetic field B_c. Above B_c, only Minkowski embedding is possible. Below B_c, metastable phases of black hole embedding are found as we increase B. We illustrate the structure of metastable phases in Fig. 5.

APPENDIX B: HYDRODYNAMIC SOLUTION OF FLUCTUATIONS

We wish to solve (27) in the hydrodynamic limit. We reproduce (27) for convenience,

$$\begin{aligned}&\omega^2\sqrt{-h}g^{tt}g_{\phi\phi}\phi-\partial_\rho(\sqrt{-h}g^{\rho\rho}g_{\phi\phi}\phi')\\&\quad-B\partial_\rho(\cos^4\theta)A_z(-i\omega)=0,\\&\omega^2\sqrt{-h}g^{tt}g^{xx}A_z-\partial_\rho(\sqrt{-h}g^{\rho\rho}g^{xx}A_z')\\&\quad+B\partial_\rho(\cos^4\theta)\phi(-i\omega)=0.\end{aligned}\tag{B1}$$

For pedagogical reasons, we work in the small B limit and solve (B1) order by order in B. Since the correction to $\sqrt{-h}$ starts from $O(B^2)$, we can simply use the $B=0$ limit of $\sqrt{-h}$ for the solution up to $O(B)$. The order $O(B^0)$ solution satisfies the homogeneous equation. In the hydrodynamic regime, the solution is given by

$$\begin{aligned}\phi^{(0)}(\rho)&=1-\frac{i\omega}{2r_0}\left[\int_1^\rho d\rho'\left(\frac{(\frac{r_0^2}{2})^2 8\cos^3\theta_h\sin^2\theta_h}{\sqrt{-h(\rho')}g^{\rho\rho}(\rho')g_{\phi\phi}(\rho')}\right.\right.\\&\quad\left.\left.-\frac{1}{\rho'-1}\right)+\ln(\rho-1)\right],\\A_z^{(0)}(\rho)&=1-\frac{i\omega}{2r_0}\left[\int_1^\rho d\rho'\left(\frac{\frac{r_0^2}{2}4\cos^3\theta_h}{\sqrt{-h(\rho')}g^{\rho\rho}(\rho')g^{xx}(\rho')}\right.\right.\\&\quad\left.\left.-\frac{1}{\rho'-1}\right)+\ln(\rho-1)\right].\end{aligned}\tag{B2}$$

We have chosen a specific normalization for the homogeneous solutions. At order $O(B)$, we need to solve the inhomogeneous equations sourced by the mixing terms. This can be achieved by using the Green's functions for ϕ and A_z, which are defined by

$$\begin{aligned}&\partial_\rho^2\mathcal{G}_\phi(\rho,\rho')+\partial_\rho\mathcal{G}_\phi(\rho,\rho')\partial_\rho\ln(\sqrt{-h}g^{\rho\rho}g_{\phi\phi})\\&\quad-\frac{\omega^2 g^{tt}}{g^{\rho\rho}}\mathcal{G}_\phi(\rho,\rho')=\delta(\rho-\rho'),\\&\partial_\rho^2\mathcal{G}_A(\rho,\rho')+\partial_\rho\mathcal{G}_A(\rho,\rho')\partial_\rho\ln(\sqrt{-h}g^{\rho\rho}g^{xx})\\&\quad-\frac{\omega^2 g^{tt}}{g^{\rho\rho}}\mathcal{G}_A(\rho,\rho')=\delta(\rho-\rho').\end{aligned}\tag{B3}$$

We require that the inhomogeneous solutions satisfy the infalling wave condition on the horizon and vanish on the boundary. It is convenient to construct the Green's function using two independent solutions satisfying the above boundary conditions. We illustrate the procedure using $\mathcal{G}_\phi$ as an example. The two independent solutions are chosen as below:

$$\begin{aligned}\phi_h&=(\rho-1)^{-\frac{i\omega}{2r_0}}(1+\cdots)=h_0+\frac{h_1}{\rho^2}+\cdots,\\\phi_b&=\phi_h h_0^*-\phi_h^* h_0=(h_0^*h_1-h_0h_1^*)\rho^{-2}+\cdots.\end{aligned}\tag{B4}$$

Here, ϕ_h satisfies the infalling wave condition on the horizon. h_0 and h_1 (not to be confused with h) are coefficients of the asymptotic expansion of ϕ_h. ϕ_b is constructed from a linear combination of ϕ_h and its complex conjugate such that it vanishes on the boundary. $\mathcal{G}_\phi$ can be constructed as follows:

$$\begin{aligned}\mathcal{G}_\phi(\rho,\rho')=&\frac{1}{\phi_b'(\rho')\phi_h(\rho')\phi_b(\rho')\phi_h{}'(\rho')}\\&\times[\phi_h(\rho')\phi_b(\rho)\theta(\rho-\rho')\\&+\phi_b(\rho')\phi_h(\rho)\theta(\rho'-\rho)].\end{aligned}\tag{B5}$$

The Wronskian appearing in (B5) can be fixed up to normalization from the homogeneous equation:

$$\phi_b'\phi_h-\phi_h'\phi_b=\frac{\#}{\sqrt{-h}g^{\rho\rho}g_{\phi\phi}}.\tag{B6}$$

We can fix the normalization by taking the limit $\rho\to\infty$ of (B6). Comparing the limit with (B4), we obtain

$$\#=\left(\frac{r_0^2}{2}\right)^2 m^2(h_0^*h_1-h_0h_1^*)(-2)h_0,\tag{B7}$$

where we used the fact $\rho\sin\theta|_{\rho\to\infty}=m$. The inhomogeneous solution is given by the convolution of the Green's function and corresponding source

$$\phi^{(1)}(\rho)=\int_1^\infty d\rho'\mathcal{G}_\phi(\rho,\rho')s(\rho'),\tag{B8}$$

with the source

$$s(\rho)=\frac{B\partial_\rho(\cos^4\theta)A_z^{(0)}i\omega}{\sqrt{-h}g^{\rho\rho}g_{\phi\phi}}.\tag{B9}$$

We are only interested in the limit $\rho\to\infty$ of (B8), which is

$$\begin{aligned}\phi^{(1)}(\rho)=&\int_1^\infty d\rho'\frac{\phi_h(\rho')B\partial_{\rho'}(\cos^4\theta(\rho'))A_z^{(0)}(\rho')i\omega}{(\frac{r_0^2}{2})^2m^2(-2)h_0}\rho^{-2}\\&+\cdots.\end{aligned}\tag{B10}$$

Following the same procedure, we obtain the counterpart of A_z,

$$A_z^{(1)}(\rho) = \int_1^\infty d\rho' \frac{-A_{z,h}(\rho')B\partial_{\rho'}(\cos^4\theta(\rho'))\phi^{(0)}(\rho')i\omega}{(\frac{r_0^2}{2}(-2)a_0)}\rho^{-2} + \cdots, \tag{B11}$$

where $A_{z,h}$ is defined as the solution satisfying the infalling wave condition on the horizon, with boundary value a_0.

Before closing this section, we claim that (B2), (B10), and (B11) can also be understood as series expansions in ω; we should discard the $O(\omega)$ terms in (B2) and view the rest as a zeroth solution. The first order solutions get contributions from the discarded terms in (B2), (B10), and (B11). Furthermore, we can allow for arbitrary dependence of $\sqrt{-h}$ on B in (B2), (B10), and (B11) provided that we work with sufficiently small ω.

[1] D. E. Kharzeev, L. D. McLerran, and H. J. Warringa, The effects of topological charge change in heavy ion collisions: "Event by event P and *CP* violation", Nucl. Phys. **A803**, 227 (2008).

[2] D. Kharzeev and A. Zhitnitsky, Charge separation induced by P-odd bubbles in QCD matter, Nucl. Phys. **A797**, 67 (2007).

[3] D. Kharzeev, Parity violation in hot QCD: Why it can happen, and how to look for it, Phys. Lett. B **633**, 260 (2006).

[4] K. Fukushima, D. E. Kharzeev, and H. J. Warringa, The chiral magnetic effect, Phys. Rev. D **78**, 074033 (2008).

[5] D. E. Kharzeev and H.-U. Yee, Chiral magnetic wave, Phys. Rev. D **83**, 085007 (2011).

[6] Y. Burnier, D. E. Kharzeev, J. Liao, and H.-U. Yee, Chiral Magnetic Wave at Finite Baryon Density and the Electric Quadrupole Moment of Quark-Gluon Plasma in Heavy Ion Collisions, Phys. Rev. Lett. **107**, 052303 (2011).

[7] D. E. Kharzeev, J. Liao, S. A. Voloshin, and G. Wang, Chiral magnetic and vortical effects in high-energy nuclear collisions—A status report, Prog. Part. Nucl. Phys. **88**, 1 (2016).

[8] J. Liao, Anomalous transport effects and possible environmental symmetry 'violation' in heavy-ion collisions, Pramana **84**, 901 (2015).

[9] X.-G. Huang, Electromagnetic fields and anomalous transports in heavy-ion collisions—A pedagogical review, arXiv:1509.04073.

[10] D. T. Son and P. Surowka, Hydrodynamics with Triangle Anomalies, Phys. Rev. Lett. **103**, 191601 (2009).

[11] Y. Jiang, X.-G. Huang, and J. Liao, Chiral vortical wave and induced flavor charge transport in a rotating quark-gluon plasma, Phys. Rev. D **92**, 071501 (2015).

[12] L. Adamczyk *et al.*, Beam-Energy Dependence of Charge Separation along the Magnetic Field in Au + Au Collisions at RHIC, Phys. Rev. Lett. **113**, 052302 (2014).

[13] B. I. Abelev *et al.*, Azimuthal Charged-Particle Correlations and Possible Local Strong Parity Violation, Phys. Rev. Lett. **103**, 251601 (2009).

[14] B. Abelev *et al.*, Charge Separation Relative to the Reaction Plane in Pb-Pb Collisions at $\sqrt{s_{NN}} = 2.76$ TeV, Phys. Rev. Lett. **110**, 012301 (2013).

[15] D. E. Kharzeev and H.-U. Yee, Anomalies and time reversal invariance in relativistic hydrodynamics: the second order and higher dimensional formulations, Phys. Rev. D **84**, 045025 (2011).

[16] E. Megias and F. Pena-Benitez, Holographic gravitational anomaly in first and second order hydrodynamics, J. High Energy Phys. 05 (2013) 115.

[17] K. Jensen, P. Kovtun, and A. Ritz, Chiral conductivities and effective field theory, J. High Energy Phys. 10 (2013) 186.

[18] A. V. Sadofyev and M. V. Isachenkov, The chiral magnetic effect in hydrodynamical approach, Phys. Lett. B **697**, 404 (2011).

[19] S. Pu, J.-H. Gao, and Q. Wang, A consistent description of kinetic equation with triangle anomaly, Phys. Rev. D **83**, 094017 (2011).

[20] J.-W. Chen, S. Pu, Q. Wang, and X.-N. Wang, Berry Curvature and Four-Dimensional Monopoles in the Relativistic Chiral Kinetic Equation, Phys. Rev. Lett. **110**, 262301 (2013).

[21] M. A. Stephanov and Y. Yin, Chiral Kinetic Theory, Phys. Rev. Lett. **109**, 162001 (2012).

[22] M. Stephanov, H.-U. Yee, and Y. Yin, Collective modes of chiral kinetic theory in a magnetic field, Phys. Rev. D **91**, 125014 (2015).

[23] D. T. Son and N. Yamamoto, Berry Curvature, Triangle Anomalies, and the Chiral Magnetic Effect in Fermi Liquids, Phys. Rev. Lett. **109**, 181602 (2012).

[24] D. T. Son and N. Yamamoto, Kinetic theory with Berry curvature from quantum field theories, Phys. Rev. D **87**, 085016 (2013).

[25] Y. Wu, D. Hou, and H.-C. Ren, The subtleties of the wigner function formulation of the chiral magnetic effect, arXiv:1601.06520.

[26] J.-W. Chen, J.-Y. Pang, S. Pu, and Q. Wang, Kinetic equations for massive Dirac fermions in electromagnetic field with non-Abelian Berry phase, Phys. Rev. D **89**, 094003 (2014).

[27] V. P. Kirilin, A. V. Sadofyev, and V. I. Zakharov, Proceedings of the 100th Anniversary of the Birth of I. Ya. Pomeranchuk, Moscow, Russia, 2013 (World Scientific, Singapore, 2014), p. 272.

[28] K. Fukushima, D. E. Kharzeev, and H. J. Warringa, Real-time dynamics of the Chiral Magnetic Effect, Phys. Rev. Lett. **104**, 212001 (2010).

[29] A. Jimenez-Alba, K. Landsteiner, and L. Melgar, Anomalous magnetoresponse and the Stückelberg axion in holography, Phys. Rev. D **90**, 126004 (2014).

[30] I. Iatrakis, S. Lin, and Y. Yin, Axial Current Generation by P-Odd Domains in QCD Matter, Phys. Rev. Lett. **114**, 252301 (2015).

[31] I. Iatrakis, S. Lin, and Y. Yin, The anomalous transport of axial charge: topological vs non-topological fluctuations, J. High Energy Phys. 09 (2015) 030.

[32] A. Jimenez-Alba, K. Landsteiner, Y. Liu, and Y.-W. Sun, Anomalous magnetoconductivity and relaxation times in holography, J. High Energy Phys. 07 (2015) 117.

[33] Y.-W. Sun and Q. Yang, Negative Magnetoresistivity in Holography, arXiv:1603.02624.

[34] C. Hoyos, T. Nishioka, and A. O'Bannon, A chiral magnetic effect from AdS/CFT with flavor, J. High Energy Phys. 10 (2011) 084.

[35] D. Mateos, R. C. Myers, and R. M. Thomson, Holographic Phase Transitions with Fundamental Matter, Phys. Rev. Lett. **97**, 091601 (2006).

[36] C. Hoyos-Badajoz, K. Landsteiner, and S. Montero, Holographic meson melting, J. High Energy Phys. 04 (2007) 031.

[37] V. G. Filev, C. V. Johnson, R. C. Rashkov, and K. S. Viswanathan, Flavoured large N gauge theory in an external magnetic field, J. High Energy Phys. 10 (2007) 019.

[38] J. Erdmenger, R. Meyer, and J. P. Shock, AdS/CFT with flavour in electric and magnetic Kalb-Ramond fields, J. High Energy Phys. 12 (2007) 091.

[39] C. Manuel and J. M. Torres-Rincon, Dynamical evolution of the chiral magnetic effect: Applications to the quark-gluon plasma, Phys. Rev. D **92**, 074018 (2015).

[40] D. Grabowska, D. B. Kaplan, and S. Reddy, Role of the electron mass in damping chiral plasma instability in Supernovae and neutron stars, Phys. Rev. D **91**, 085035 (2015).

[41] G. Basar and D. E. Kharzeev, The Chern-Simons diffusion rate in strongly coupled N = 4 SYM plasma in an external magnetic field, Phys. Rev. D **85**, 086012 (2012).

[42] T. Drwenski, U. Gursoy, and I. Iatrakis, Thermodynamics and *CP*-odd transport in Holographic QCD with Finite Magnetic Field, arXiv:1506.01350.

[43] A. Karch, A. O'Bannon, and E. Thompson, The stress-energy tensor of flavor fields from AdS/CFT, J. High Energy Phys. 04 (2009) 021.